Experimental and Simulation Studies on Magnetic Nanoparticle Assembly for Scalable Polymer Nanocomposite Fabrication

Mychal P. Spencer[1], David Gao[2], and Namiko Yamamoto[3]
The Pennsylvania State University, University Park, PA, 16802

The magnetic assembly of nanoparticles is a promising technique for the scalable manufacturing of tailored polymer nanocomposites. Tailored nanostructure assembly can lead to improvements in thermal, electrical, and mechanical properties of polymer nanocomposites, but it is currently difficult to achieve hierarchical morphologies of the nanoparticles. The usage of magnetic fields is a useful method to control nanoparticle assembly since it allows the bulk processing of polymer nanocomposites, while still retaining nanostructures across the large volume. Further studies are necessary for the control over magnetic nanoparticle assembly due to uncertainties in parametric variations. This work presents continued experimental and new theoretical work on nanoparticle assembly using oscillating magnetic fields. In the last 2016 SciTech/AIAA SDM conference, experimental parametric studies were presented about the effects of the magnetic flux density, frequency, and concentration on the nanoparticle structuring.[20] In this work, the effects of additional parameters of the applied magnetic fields (the waveform type and low frequencies) and the nanoparticles (magnetic properties and size) were investigated. In order to understand the experimentally observed trends, simulations are being performed using COMSOL Multiphysics Modeling Software, particularly on the interactions between particles. Our results demonstrate that frequencies as low as 0.04 Hz can provide significant tailorability to nanoparticle assemblies. In addition, a sinusoidal waveform is found to provide even more tailorability at low frequencies compared to a square waveform. The influence particle size is apparent; larger and more homogenous nanoparticle assemblies are found for increasing particle size. In simulations, a magnetic threshold length was calculated as a function of particle orientation and separation; when the nanoparticles are separated beyond the threshold length, nanoparticle assembly does not occur due to hydrodynamic forces. The understanding of the underlying assembly mechanisms will help evaluation of the scalability of manufacturing a tailored polymer nanocomposite using an oscillating magnetic field. In near-future, fabrication of coupon-sized, thin polymer nanocomposites will be demonstrated using a scaled-up magnetic assembly set-up.

Nomenclature

B	=	magnetic flux density
μ	=	magnetic moment
η	=	dynamic viscosity
r_p	=	particle radius
m_p	=	particle mass
x	=	particle x-direction displacement
t	=	time
T	=	Maxwell's stress tensor

I. Introduction

POLYMER nanocomposites are an important research topic[1] since their microstructures can be tailored providing high mechanical rigidity,[2] thermal insulation,[3] radiation shielding,[4] and more.[5-7] Previously, polymer nanocomposites were created by directly mixing the nanoparticles into the polymer matrix which produced nonhomogeneous particle distributions and even degraded mechanical properties.[8-10] An active assembly manufacturing methodology using oscillating magnetic fields is investigated in this work in order to achieve bulk and

[1]Graduate Research Assistant, Aerospace Engineering, 229 Hammond, University Park, PA 16802, Student Member
[2]Undergraduate Research Assistant, Aero. Engr., 229 Hammond, University Park, PA 16802, Student Member
[3]Assistant Professor, Aerospace Engineering, 232A Hammond, University Park, PA 16082, Member

ordered nanoparticle organization. Active assembly using oscillating magnetic fields is a promising technique since it allows for the bulk processing of nanocomposites while retaining a homogeneous microstructure. The assembly of magnetic nano- or microparticles in a static magnetic field has been studied extensively in the past, mostly in terms of the treatment and separation of cells.[11-14] Oscillating magnetic fields have been used to evaluate the bulk alignment of microparticles (such as rods, platelets, etc.) leading to novel mechanical properties.[15-19] However, information regarding the assembly of nanoparticles under the influence of oscillating magnetic fields is missing.

This work presents continued experimental and new theoretical work on nanoparticle assembly using oscillating magnetic fields. In the last 2016 SciTech/AIAA SDM conference, experimental parametric studies were presented about the effects of the magnetic flux density, frequency, and concentration on the nanoparticle structuring.[20] In this work, the effects of additional parameters of the applied magnetic fields (the waveform type and low frequencies) and the nanoparticles (magnetic properties and size) will be investigated. In order to understand the experimentally observed trends, simulations are being performed using COMSOL Multiphysics Modeling Software, particularly on the interactions between particles. The understanding of the underlying assembly mechanisms will help evaluation of the scalability of manufacturing a tailored polymer nanocomposite using an oscillating magnetic field. In near-future, fabrication of coupon-sized, thin polymer nanocomposites will be demonstrated using a scaled-up magnetic assembly set-up.

II. Materials and Methods

A. In-situ observation of magnetic nanoparticle assembly

The magnetic assembly of nanoparticles in deionized water are studied. The details of the magnetic assembly processes are given in the previous conference paper.[20] Iron oxide solutions are diluted in deionized water to two different concentrations (1 and 2 mg per ml). Three types of iron oxide nanoparticles are used in this work:

1. Spherical, superparamagnetic particles (Sigma-Aldrich, I7643, ~20 nm diameter) supplied in an aqueous suspension (50 mg per ml in 1 mM EDTA, pH 7.0) which are amine-terminated to maintain particle suspension, see Figure 1;
2. Spherical particles (US Research Nanomaterials, US7558, Fe_2O_3-γ, ~ 35 nm diameter) supplied at 10% weight in water;
3. Spherical particles (US Research Nanomaterials, US7568, Fe_3O_4, ~ 25 nm diameter) supplied at 20% weight in water.

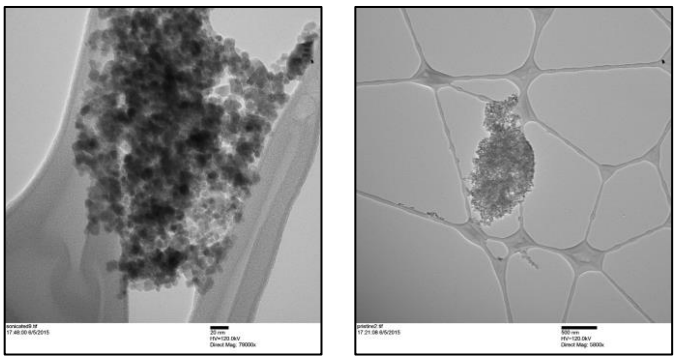

Figure 1. TEM images of the superparamagnetic iron oxide nanoparticle agglomerations. The scale bar is 20 nm and 500 nm for the left and right image, respectively.

The solutions are encapsulated in a KOVA Glasstic slide with a height of 0.1 mm and a chamber volume of 6.6 μL, and then are mounted between a pair of solenoids. Images are collected using an optical microscope at 0, 5, 10, and 15 minutes with 15 minutes representing magnetic saturation (defined as the time when the particle structuring is nearly constant). Two different waveform types are investigated in this work: a 50% duty cycle square waveform with magnetic flux density amplitudes of 50 G and 100 G and a sinusoidal waveform with root-mean-square (RMS) magnetic flux densities of 50 G (70.7 G peak) and 100 G (141.4 G peak). A minimum magnetic flux density of 50 G is selected to ensure structuring above the magnetic threshold, and the low frequency range (< 5 Hz) is investigated based on previous work.[20]

The optical microscope images are processed using Matlab to quantitatively evaluate particle morphology. Due to settling, the area fraction of the nanoparticles in the microscope images are much greater than the volume fraction

of the overall samples. For example, at a volume fraction of 0.06% (or a concentration of 4 mg per ml for I7643), an area fraction of greater than 10% is found in the processed images. Due to intermolecular attraction, images of the particle dispersions at 0 minutes show initial groupings greater than 1 μm in size (see Figure 2). When the magnetic field is applied, the particles form particle agglomerations or *clusters* aligned along the direction of the magnetic field. An analysis code is used to evaluate the average cluster size, length, width, and separation to parametrically understand nanoparticle structuring for different input parameters (magnetic flux density, waveform, concentration, and frequency), as shown in Figure 3.

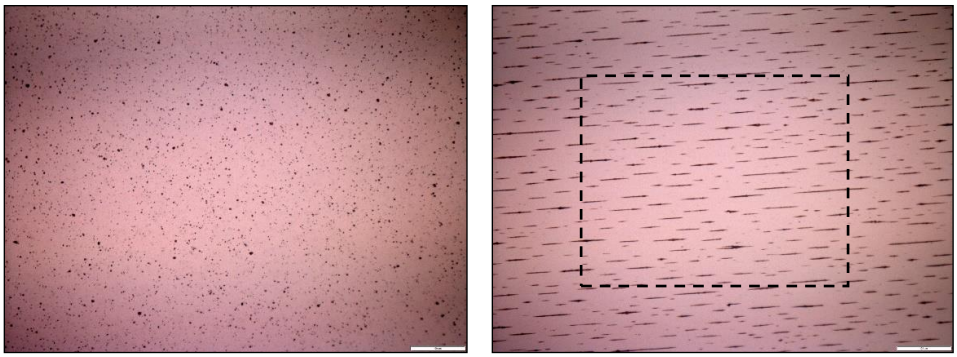

Figure 2. Optical microscope images of nanoparticle suspension (Sigma-Aldrich I7643) prior to application of magnetic field (left) and application of ± 50 G, 0.1 Hz square waveform for 15 minutes (right). The scale bar is at 100 μm.

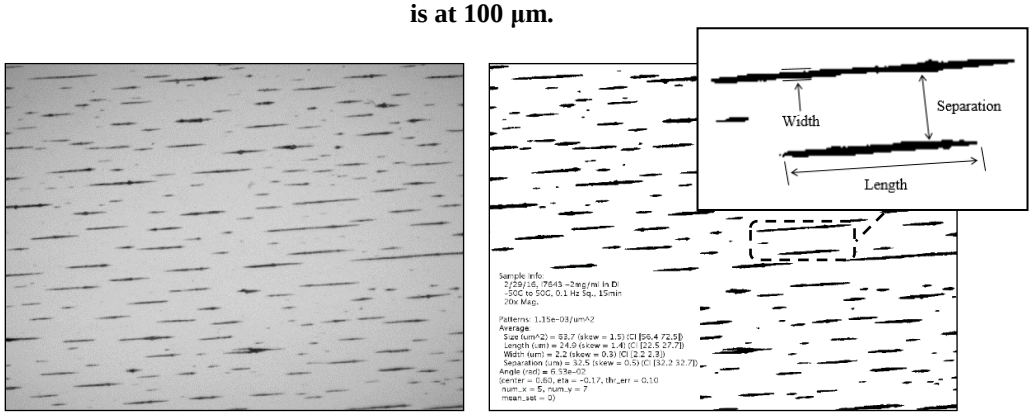

Figure 3. (Left) Selected region of the optical microscope image as shown by the box in Figure 2 (right) to analyze with the Matlab code. (Right) Quantitative analysis of the particle structuring. The insert depicts the defined structuring characteristics.

B. Theoretical studies on magnetic assembly of nanospheres

Magnetic assembly of nanoparticles are also studied using COMSOL Multiphysics Modeling Software. During assembly, the nanoparticles are acted upon by five forces: (1) the force due to the external magnetic field, (2) the particle-to-particle interaction forces including magnetic and van der Waals forces, (3) hydrodynamic loadings such as drag, (4) thermal energy effects, and (5) Brownian motion. Due to the initial nanoparticle agglomerations being on the order of 1 μm in size or greater, see Figure 2, the effects of thermal energy and Brownian motion on the motion of the nanoparticle clusters are negligible. In addition, previous findings using Sigma-Aldrich I7643 have shown that initial nanoparticle agglomerations disperse or diffuse upon removal of the external magnetic field indicating that intermolecular forces at the micron scale, such as van der Waal forces, are less dominant than the forces induced by the applied magnetic fields. Therefore, three primary forces are selected to model the structuring of the nanoparticle clusters: the external magnetic field, magnetic particle-to-particle interactions, and hydrodynamics.

The COMSOL simulations are currently performed to model a simplified two-dimensional case of magnetic dipoles under a constant (DC) and uniform magnetic field application. The classic governing equation of a force acting on a magnetic dipole is given in Eq. (1),[21,22] where B is the magnetic flux density and μ is the magnetic moment. When a point-like dipole is assumed (for example, a superparamagnetic particle), then the space gradient of the magnetic moment is zero, $(\nabla \times \vec{\mu}) = 0$ and $(\nabla \vec{\mu}) = 0$. For a static field, free of current sources (a so-called source free field),

Maxwell's forth equation can be reduced to Eq. (2).[23] Therefore, the magnetic force acting on a superparamagnetic particle in an external magnetic field can be simplified to Eq. (3), which indicates that the net force acting on a superparamagnetic particle is zero if no gradient exists in the magnetic flux density. Thus, in the presence of a uniform and static magnetic field, the only force assisting agglomeration of superparamagnetic particles are the magnetically induce dipole-dipole forces due to particle magnetization. The COMSOL simulations are performed to verify no particle motion of a single particle in a static or DC magnetic field, and to model the attraction between two particles in a DC field due to a non-uniform magnetic field generated between the particles by particle magnetization (the so-called particle-to-particle magnetic interaction).

$$\vec{F}_m = \nabla\left(\vec{\mu}\cdot\vec{B}\right) = (\vec{\mu}\cdot\nabla)\vec{B} + \vec{\mu}\times\left(\nabla\times\vec{B}\right) + \vec{B}\times(\nabla\times\vec{\mu}) + \left(\vec{B}\cdot\nabla\right)\vec{\mu} \tag{1}$$

$$\left(\nabla\times\vec{B}\right) = 0 \tag{2}$$

$$\vec{F}_m = (\vec{\mu}\cdot\nabla)\vec{B} \tag{3}$$

In the simulation, idealized circular, isotropic iron particles are used for simplicity; the relative magnetic permeability is set as 30000. The particles are placed within water and the domain length and particle radius are selected to be 1000 μm and 20 μm, respectively. The magnetic fields, global ODEs, and moving mesh interfaces are coupled to simulate motion of magnetic particles; the force acting on the particle is solved via the magnetic fields interface using the Maxwell stress tensor. Automatic remeshing is enabled to ensure no mesh distortion. A summary of the simulation domain is shown in Figure 4. The simulation is set-up using the following procedure:

i. Create the geometry.
   a. Define the fluid domain length (1000 μm).
   b. Define the particle size (20 μm radius) and placement.
   c. Specify an infinite domain around the fluid domain.
ii. Specify the materials properties for the fluid and particles.
iii. Add a global ODE module.
   a. For each particle, specify the equations of motion.
   b. The equation of motion incorporating Stokes' drag and magnetic force is shown in Eq. (4) for the x-direction, where η is the dynamic viscosity, r_p is the particle radius, m_p is the particle mass, x is the particle displacement in the x-direction, t is the time, and T_x is the resulting force on the particle in the x-direction due to integration of Maxwell's stress tensor over the particle surface.

$$6\pi\eta r_p\frac{dx}{dt} + m_p\frac{d^2x}{dt^2} - T_x = 0 \tag{4}$$

   c. For example, in the x-direction, the inputted ODE into COMSOL would appear as shown in Eq. (5), where xp1 is the particle name, xp1t and xp1tt are first and second derivatives of xp1 with respect to time, and *mf1.Forcex_F1* is the COMSOL magnetic fields interface (*mf1*) x-direction force (*Forcex*) for particle 1 (*F1*).

$$6\pi\eta r_p(xp1t) + m_p(xp1tt) - mf1.Forcex\_F1 = 0 \tag{5}$$

iv. Add a moving mesh (ALE) module.
   a. Fix the infinite domain.
   b. Specify zero mesh displacement at the domain boundary.
   c. Select free deformation for the fluid domain.
   d. For each particle in the domain, specify a prescribed deformation as the x- and y-displacements solved for by the ODE.
   e. For each particle in the domain, specify a prescribed mesh displacement at the particle boundaries as the x- and y-displacements solved for by the ODE.
v. Add a magnetic fields interface module.
   a. Create the desired magnetic field (in this case, a uniform DC field).
   b. Calculate the forces acting on each particle (which will couple with the ODE).

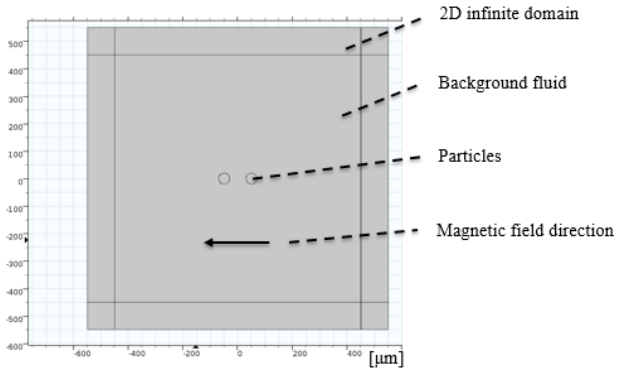

Figure 4 – The particle geometry and domain for the COMSOL simulation.

III. Results and Discussion

A. Experimental studies of magnetic assembly

Previous work by the authors[20] demonstrated the dependence of particle structuring on the magnetic flux density, frequency, and concentration. A very low frequency (< 1 Hz) led to a significant change in the average separation between clusters, an increase in the magnetic flux density increased the average length and reduced the average width of the clusters, and an increase in the concentration produced larger clusters on average. In this work the parametric trends are investigated for a lower frequency range, two waveforms types (square vs. sinusoidal), and larger particle sizes.

Tests are conducted using superparamagnetic nanoparticles I7643 (2 mg per ml) at 50 G to determine cluster morphology changes at very low frequencies. Results demonstrate a significant change in the average cluster size, length, and separation for frequencies below 0.3 Hz, as shown in Figure 5. The average cluster size increases by ~84% and the average length increases by ~70%, when the frequency was increase from 0 Hz (DC) to 0.04 Hz. This result is consistent with the previous findings[20] that a very small frequency increase from 0 Hz can produce significant changes in the cluster geometries due to the directional change of the magnetic moment which produces additional particle-to-particle attraction forces. Beyond 0.3 Hz, the cluster properties plateau due to a limiting time response of the nanoparticles magnetic moment.

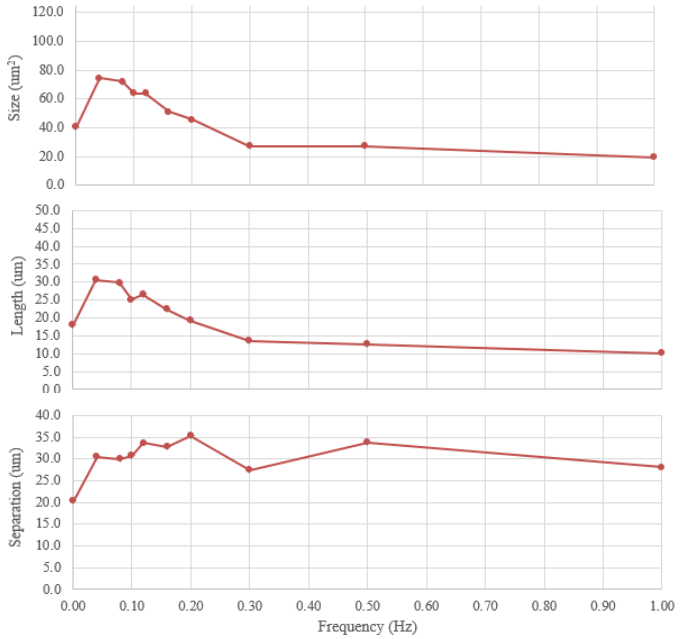

Figure 5. The effects of magnetic field frequency on nanoparticle structuring. The top, middle, and bottom images present the average size, length, and separation of the clusters, respectively. Tests were conducted using superparamagnetic nanoparticles I7643 at 50 G and 2 mg per ml.

Assembly with sinusoidal magnetic waves are performed using superparamagnetic nanoparticles I7643 (1 mg per ml) with a magnetic flux density of 50 G RMS and 100 G RMS. The effect of the waveform was apparent at very low frequencies; the sinusoidal waveform resulted in a greater change in the cluster properties than the square waveform, and its degree became more significant in the low frequency and high magnetic flux density ranges. The trends observed are similar to those found previously with the square magnetic waves.[20] However, at a magnetic flux density of 100 G RMS, the average cluster size increases by ~110 % and separation increases by ~140%, when the field frequency increases from 0 Hz (DC) to 0.10 Hz (see Figure 6). These feature size increases are larger than the previous case with the square magnetic waves: ~100 % increase of size and ~33% increase of separation for I7643 (2 mg per ml) at 100 G square field with a field frequency increase from 0 Hz (DC) to 0.10 Hz; the concentration difference is assumed not to significantly alter the findings since previous tests have shown that changes in concentration produce a maximum 10% change in the size and separation of the clusters from a DC to 0.10 Hz field. It is hypothesized that at very low frequencies the magnetic moment of the particles is able to respond to the continuously changing external magnetic field, as opposed to a square waveform which only produces an external magnetic field gradient over small time intervals. This gradient in the magnetic moment is likely responsible for additional particle-to-particles forces, increasing the cluster geometry feature sizes. When frequency further increases, the response of the particles magnetic moment cannot catch up with the fast changes of the external magnetic field, and becomes limited; the sinusoidal results converge to those found for the square waveform for the higher frequency range (> 1.0 Hz). These results indicate that a continuous waveform in the low frequency regime can potentially provide more tailorability of nanoparticles patterns. Further studies are necessary before deducing conclusions, especially on the effect of hydrodynamic forces from polymer matrix viscosity.

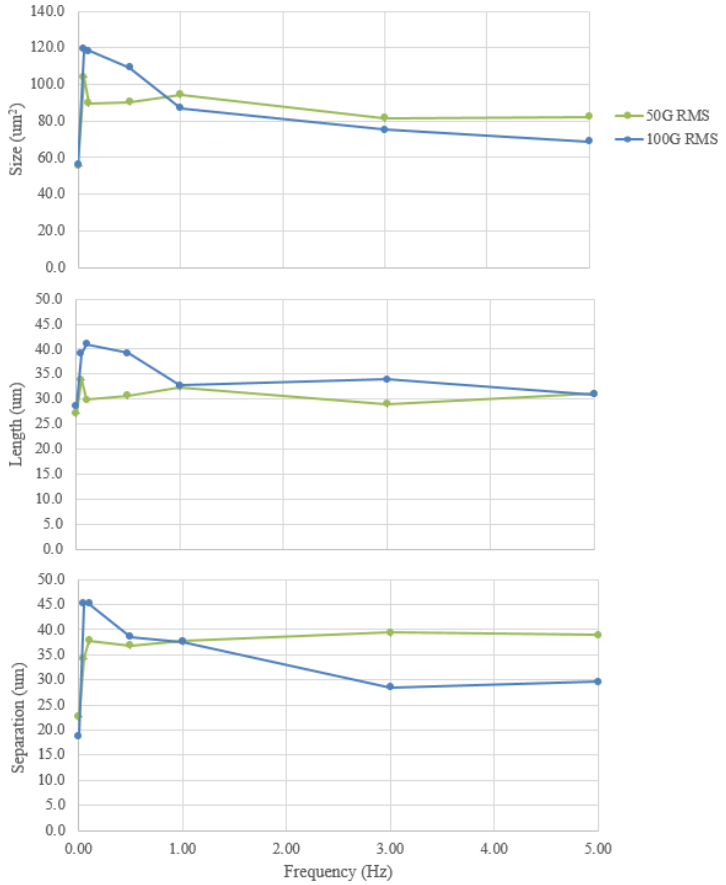

Figure 6. The effect of a sinusoidal waveform on the structuring characteristics of nanoparticles. The top, middle, and bottom image represent the average size, length, and separation of the clusters, respectively.

The applicability of the superparamagnetic trends to different particle types is of interest for validation, and future dispersions in polymer matrices. Tests are conducted using iron oxide nanoparticles (as supplied by US Research Nanomaterials) at two different particle sizes – (1) Fe_2O_3-γ at 35 nm, and (2) Fe_3O_4 at 25 nm. As shown by Figure 7, with a DC magnetic field, thin and long clusters are formed along the direction of the magnetic field, similar to previously demonstrated results.[20] The larger particle, Fe_2O_3-γ, produces a notably larger cluster size, with fewer clusters in the imaging region, due to the increased magnetization of the particles, and thus stronger magnetic dipole-dipole interaction forces. Upon application of a very low frequency component, the separation between the clusters increases, in agreement with trends found for superparamagnetic particles. While not shown, the influence of the magnetic flux density is noticeable – increases in the magnetic flux density produced significantly longer, and more homogenous, clusters, in agreement with previous trends.[20] Additional work is being conducted with larger-sized nanoparticles to determine the influence on cluster morphology in polymer matrices.

Fe_2O_3-γ at DC

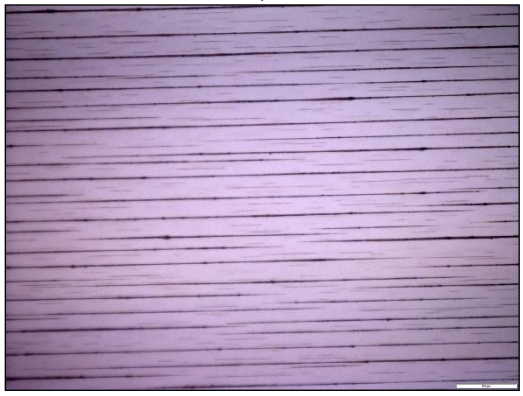

Fe_3O_4 at DC

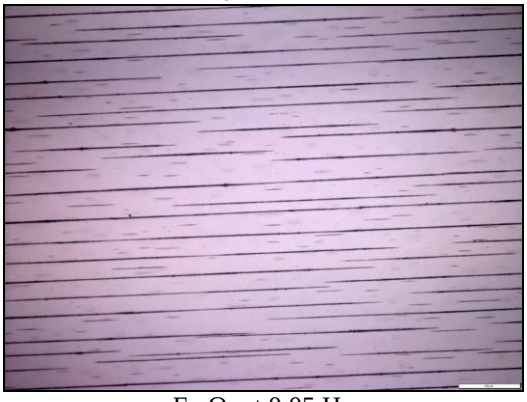

Fe_3O_4 at 0.05 Hz

Figure 7 – Parametric verification of cluster morphology variations for Fe_2O_3-γ and Fe_3O_4. Results are shown for 2 mg/ml, 100 G, and at 5 minutes. The scale bar is 100 μm.

B. Theoretical studies of magnetic assembly

The COMSOL simulations are currently performed for a simplified two-dimensional case of magnetic dipoles under a constant (DC) magnetic field. A simulation is first performed for a single iron particle (20 μm radius, relative permeability of 30,000) to verify no motion of the particle in a DC magnetic field (as would be expected from a magnetic dipole, see Eq. (3)). As shown in Figure 8, the particle does not displace in a DC magnetic field (50 G), verifying Eq. (3) since there is no gradient in the magnetic flux density and the resulting magnetic force is approximately zero. Then, two particles (20 μm radius, relative permeability of 30,000) are placed in the DC magnetic field at different angular positions and separations in order to simulate particle-to-particle magnetic interactions. Due to the magnetization of the particles, a gradient in the magnetic flux density is produced between the particles leading to attraction or repulsion. Attraction between the particles is enhanced when the particles are placed horizontal, similar to the finding that particle clusters tend to attach head-to-tail forming long chains along the magnetic field direction.

As shown in Figure 9, there exists a threshold length; at a DC magnetic field of 50 G, if the distance between the particles is larger than the threshold length of approximately 190 μm, the two particles do not attract or attract at an extremely slow rate due to weak interparticle forces which is a function of interparticle distance and also of the magnetic field and the fluid viscosity. The particles are required to be closer in order to attract the more vertical their alignment becomes, and when the particles do attract they attach in the direction of the external magnetic field. Additional simulations are being investigated to determine the influence of viscosity on the attraction time, the interaction between several particles of different size and shape, and modeling the influence of frequency on particle attraction.

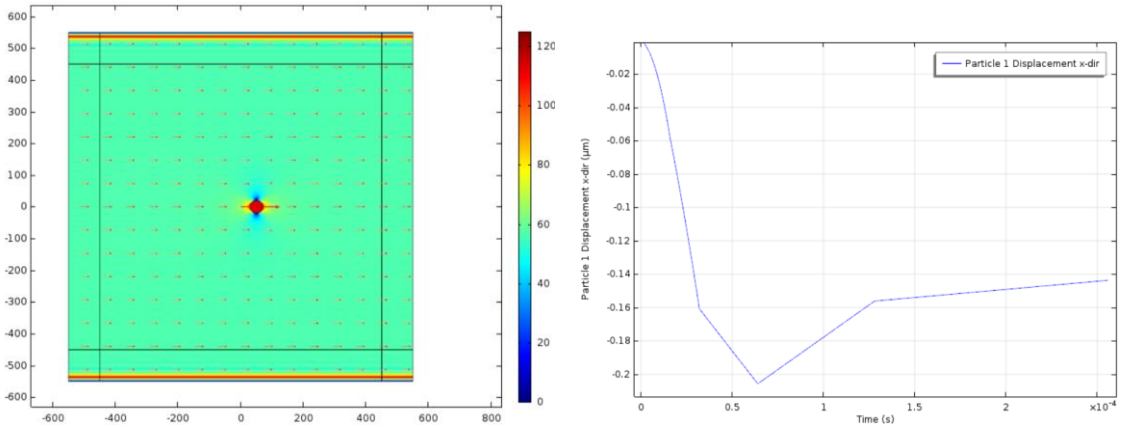

Figure 8. The magnetization (left) of one iron particle in a DC magnetic field of 50 G; the vectors represent the direction of the magnetic field and the legend represents the magnetic flux density in Gauss. The displacement (right) of the iron particle with respect to time.

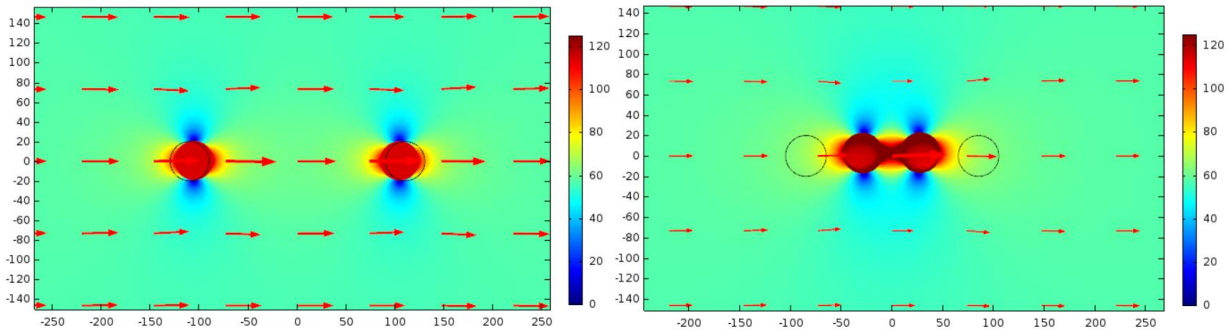

Figure 9. The attraction between two iron particles at 220 μm (top) and 170 μm (bottom) separation. The vertical and horizontal axis are in μm and the legend is in Gauss.

IV. Conclusion

An improved parametric understanding of morphology variations of nanoparticle assemblies is required for tailored polymer nanocomposite fabrication. We have previously demonstrated that effective alignment of nanoparticle assemblies occurs along magnetic field lines and depends on parameters such as magnetic flux density, magnetic field frequency, and nanoparticle concentration.[20] In this work, we have shown that nanoparticle assembly morphology is also dependent upon the magnetic field waveform; a sinusoidal waveform significantly increases assembly tailorability at very low frequencies (< 0.1 Hz) when compared to a square waveform. While the influence of frequency on assembly morphology was previously investigated, nanoparticle assembly at ultra-low frequencies is of interest for the low power tailoring of polymer nanocomposites. We have demonstrated that an ultra-low frequency component (0.04 Hz) produces the most significant variation in assembly morphology, leading to the hypothesis of the existence of a cut-off frequency. Below the cut-off frequency, morphology changes do not occur and assembly morphology is similar to that found for static or DC fields. Above the cut-off frequency, the largest variation in nanoparticle assembly morphology occur. Parametric verification of morphology trends is important for future dispersions of nanoparticles into polymer matrices. We have shown that previously demonstrated morphology trends for magnetic flux density and frequency are valid for nanoparticles with larger radii and different magnetic responses. In addition, the size of the nanoparticle was found to have a correlation to the size and homogeneity of the nanoparticles assemblies. Lastly, simulation results agreed with basic mechanisms for particle-particle magnetic attraction observed in experiments, and provide a foundation for more complicated analysis. Future work includes tailoring cluster morphology in polymers with a 1D and 2D magnetic field, in addition to material characterization. The simulation conditions will be updated to create a model which is more comparable with our experiments.

Acknowledgements

This work was supported by the Office of Naval Research, Grant No. N00014161217, the Hartz Family Career Development Professorship in Engineering, and the Pennsylvania State University (PSU) Department of Aerospace Engineering.

References

[1]Meador, M.A., Files, B., Li, J., Manohara, H., Powell, D., and Siochi, E.J., "NASA Nanotechnology Roadmap – Technology Area 10," NASA, 2012.

[2]Mansoori, G.A., "Advances in Atomic and Molecular Nanotechnology," In Nanotechnology: The emerging cutting-edge technology, UN-APCTT Tech Monitor, 2002, pp. 53-59.

[3]Yamamoto, N., Gdoutos, E., Toda, R., White, V., Manohara, H., and Daraio, C., "Thin Films with Ultra-Low Thermal Expansion," Adv. Mater. 26, 2014, pp. 3076-3080.

[4]"National Nanotechnology Initiative – Leading to the Next Industrial Revolution," Microscale Thermophysical Engineering, 2010, pp. 205-212.

[5]Ahir, S.V. and Terentjev, E.M., "Photomechanical Actuation in Polymer-Nanotube Composites," Nature Materials 4, 2005, pp. 491-495.

[6]Pulickel, M.A., Schadler, L.S., and Braun, P.V., *Nanocomposite Science and Technology*, Wiley-VCH, Weinheim, Germany, 2003.

[7](Editors) Chou, T.W. and Sun, C.T., "Series on Advances in Composite Materials Volume 2: Nanocomposites," Am. Soc. for Composites, DEStech Publications, Lancaster, PA, 2012.

[8]Thostenson, E.T., Li C., and Chou, T-W., "Review – Nanocomposites in Context," Comp. Sci. Tech. 65, 2005, pp. 491-516.

[9]Moniruzzaman, M. and Winey, K.I., "Polymer Nanocomposites Containing Carbon Nanotubes," Macromolecules 39, 2006, pp. 5194-5205.

[10]Song, Y.S. and Youn, J.R., "Influence of Dispersion States of Carbon Nanotubes on Physical Properties of Epoxy Nanocomposites," Carbon 43, 2005, pp. 1378-1385.

[11]Valberg, P.A. and Butler, J.P., "Magnetic Particle Motions Within Living Cells – Physical Theory and Techniques," J. Biophysical Soc. 52, 1987, pp. 537-550.

[12]Yellen, B.B., Erb, R.M., Son, H.S., Hewlin, R., Shange, H., and Lee, G.U., "Traveling Wave Magnetophoresis for High Resolution Chip Based Separations," Lab Chip 7, 2007, pp. 1681-1688.

[13]Miltenyi, S., Muller, W., Weichel, W., and Radbruch, A., "High Gradient Magnetic Cell Separation With MACS," Cytometry 11, 1990, pp. 231-238.

[14]Jordan, A., Scholz, R., Wust, P., Fahling, H., and Felix, R., "Magnetic Fluid Hyperthermia (MFH): Cancer Treatment with AC Magnetic Field Inducted Excitation of Biocompatible Superparamagnetic Nanoparticles," J. Magnetism and Magnetic Mat. 201, 1998, pp. 413-419.

[15]Libanori, R., Erb, R.M., and Studart, A.R., "Mechanics of Platelet-Reinforced Composites Assembled Using Mechanical and Magnetic Stimuli," ACS Appl. Mater. Interfaces 5, 2013, pp. 10794-10805.

[16]Erb, R.M., Segmehl, J., Charilaou, M., Loffler, J.F., Studart, A.R., "Non-Linear Alignment Dynamics in Suspensions of Platelets under Rotating Magnetic Fields," Soft Matter 8, 2012, pp. 7604-7609.

[17]Garmestani, H., Al-Haik, M.S., Dahmen, K., Tannenbaum, R., Li, D., Sablin, S.S., and Hussaini, M.Y., "Polymer-Mediated Alignment of Carbon Nanotubes under High Magnetic Fields," Adv. Mat. 15, 2003, pp. 1918-1921.

[18]Hong, C.Y., Horng, H.E., Kuo, F.C., Yang, S.Y., Yang, H.C., and Wu, J.M., "Evidence of Multiple States of Ordered Structures and a Phase Transition in Magnetic Fluid Films Under Perpendicular Magnetic Fields," App. Phy. Let. 75, 1999, pp. 2196-2198.

[19]Erb, R.M., Libanori, R., Rothfuchs, N., and Studart, A., "Composites Reinforced in Three Dimensions by Using Low Magnetic Fields," Science 335, 2012, pp. 199-204.

[20]Spencer, M.P. and Yamamoto, N., "Nanoparticle Alignment using Oscillating Magnetic Fields for Scalable Nanocomposite Manufacturing," AIAA SciTech 2016, San Diego, CA, Jan. 4-8, 2016.

[21]Shevkoplyas, S. S., Siegel, A. C., Westervelt, R. M., Prentiss, M. G., and Whitesides, G. M., "The force acting on a superparamagnetic bead due to an applied magnetic field," Lab Chip 7, 2007, pp. 1294-1302.

[22]Jackson, K., "Magnetostatic modeling for microfluidic design," Thesis, California Polytechnic State University, June 2011.

[23]Schaller, V., Kraling, U., Rusu, C., Petersson, K., Wipenmyr, J., Krozer, A., Wahnstrom, G., Sanz-Velasco, A., Enoksson, P., and Johansson, C., "Motion of nanometer sized magnetic particles in a magnetic field gradient," J. App. Phys. 104, 2008.